Heliyon 10 (2024) e36117

Contents lists available at ScienceDirect

Heliyon

journal homepage: www.cell.com/heliyon

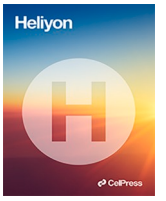

Research article

Investigation of the surface charge behaviour of ettringite: Influence of pH, calcium, and sulphate ions

Tiziana Missana *, Oscar Almendros-Ginestà, Francisco Colmenero, Ana María Fernández, Miguel García-Gutiérrez

CIEMAT, Nuclear Fission Department, Spain

ARTICLE INFO

Keywords:
Ettringite
ζ-potential
Adsorption
Double layer model
Cement

ABSTRACT

Ettringite is an important mineral that contributes to the overall performance of cementitious materials. Knowledge of the surface charge behaviour of a solid is necessary for a mechanistic description of surface processes such as adsorption or particle-particle interactions. The objective of this study was to develop a model capable of reproducing ettringite surface charge as a function of calcium, sulphate, and pH.

Ettringite was synthesised and characterised using different analytical, microscopic, and spectroscopic techniques with the help of density functional theory. Electrophoretic mobility was measured using laser Doppler electrophoresis in alkaline waters representative of the cementitious environment.

The behaviour of the ettringite surface charge was shown to be quite complex as sulphate and calcium acted in a competitive manner on the overall charge. The ζ-potential increases when the calcium content increases, whereas it decreases when sulphate increases. This is due to the possible adsorption of these ions at the surface, and the extent of the effect depends on the relative concentrations of Ca and SO_4^{2-}.

An electrostatic double layer model (DLM) was used to calculate the surface potential, considering the adsorption of both calcium and sulphate, as possible ions determining the potential (IDP), and formation of different complexes with ettringite surface functional groups (SOH). The variations of the ζ-potential could be satisfactorily predicted under the different chemical conditions of interest in a cementitious environment.

1. Introduction

Ettringite is a calcium trisulfoaluminate mineral ($Ca_6Al_2(SO_4)_3(OH)_{12}{\cdot}nH_2O$ n = 24–27), with a columnar structure, which crystallises in the trigonal system (*P*31*c*) [1,2]. It is an important hydration product of Portland cement pastes such as calcium silicate hydrates (CSH) and portlandite.

In the early stages of cement hydration, ettringite plays a role in the setting and hardening of cement [3]. Ettringite formation in the early stages of cement hydration is beneficial; however, delayed ettringite formation, often triggered by factors such as sulphate intrusion, can result in significant mineral expansion and subsequent cracking of the concrete, impacting its durability and performance [4].

* Corresponding author.
E-mail address: tiziana.missana@ciemat.es (T. Missana).

https://doi.org/10.1016/j.heliyon.2024.e36117
Received 4 April 2024; Received in revised form 22 July 2024; Accepted 9 August 2024
Available online 13 August 2024

The surface charge of a solid is linked to its chemical environment and plays a pivotal role in governing surface phenomena, such as particle aggregation and dispersion, crystal growth, and interactions with solute ions. Furthermore, cement is commonly used as a barrier material in radioactive waste disposal [5]. Therefore, the improvement of predictive models for contaminant retention is vital for assessing the safety of these systems. Thus, knowledge of surface charge behaviour and the capability to reproduce it through geochemical modelling, by varying the main solute properties, is crucial for describing surface processes, particularly adsorption. Additionally, surface charge affects particle-particle interactions and particle growth, which may contribute to cement deterioration due to sulphate presence and ettringite modifications [6,7].

First attempts to measure ettringite surface charge through electrophoretic measurements (ζ-potential) were conducted by Chen & Mehta [8], who concluded that ettringite carries a negative charge. Plank & Hirsch [9] analysed the ζ-potential of ettringite in the early cement hydration phases and concluded that it is positive. Medala et al. [10] studied the surface charge of ettringite and modelled the experimental data using Monte Carlo simulations, deducing that sulphate is the unique ion determining the potential (IDP) of the mineral (even observing positive ζ-potential under certain experimental conditions). This is in apparent contradiction to a previous study by Pointeau et al. [11] who reported an increase in the electrokinetic potential when increasing the $Ca(OH)_2(aq)$ concentration in the system, assuming Ca as the IDP.

No attempts have been made to understand the reasons for the different behaviours observed, and, to the best of our knowledge, no previous studies have been dedicated to developing a surface model that can explain the variation in the electrostatic surface potential as a function of pH, calcium, and sulphate content.

Analysis of the surface charge and its ability to describe it under variable chemical conditions is a fundamental step in understanding surface processes and interactions with solutes, including adsorption. In the context of radioactive waste repositories, where adsorption is considered a fundamental process for safety assessment, ettringite has been regarded as a mineral of interest due to its ability to adsorb both anionic and cationic species [3,12–18]. Nonetheless, geochemical modelling of sorption processes that account for the main chemical variables has not yet been reported due to the lack of a surface charge model.

Thus, the main objectives of this study are: 1) to analyse the mechanisms driving the surface charge of ettringite under alkaline conditions, enhancing the understanding of its behaviour across various stages of cement degradation, and 2) to develop a simple model that accurately reproduces the ettringite surface charge under chemical conditions relevant to cementitious environments, and to improve the description of ettringite's surface interactions with solutes.

The origin of the surface charge of a mineral depends on the nature of the surface and the chemistry of the contact water. The charge behaviour of natural materials, such as clays or oxides, has been widely described in the literature. Clay minerals have a structural negative charge which is compensated for by the adsorption of cations in the interlayer. The excess negative charge, called cation exchange capacity (CEC), can be determined using various experimental methods [19]. The cation exchange process does not imply charge variation.

Oxides possess surface functional groups, typically denoted as =SOH groups, which can be protonated or deprotonated, resulting in positively charged ($=SOH_2^+$) or negatively ($=SO^-$) charged groups. The charge of these groups primarily depends on the pH of the contacting solution. For oxides, H^+ is the main IDP and the surface charge (σ_0) is calculated considering the difference between the concentrations of positively and negatively charged surface sites [$= SOH_2^+$] - [$= SO^-$]. In a double-layer approximation, the relationship between the surface charge and potential is described by the Gouy-Chapman equation [20]. The complexation or specific adsorption of anions or cations at these sites, particularly at sufficient concentrations, may alter the initial surface charge.

Potentiometric titrations are commonly used to determine parameters such as surface site density or protonation/deprotonation constants that control the surface charge of oxides or materials with oxide-like surface functional groups. However, for cementitious minerals, which can exist only under specific chemical conditions (e.g., pH or Ca/Si content) and are influenced by dissolution/precipitation processes, potentiometric titrations are not applicable. Moreover, concepts such as the "point of zero charge" may not be directly relevant in this context. Consequently, alternative approaches are required.

Almendros-Ginestà et al. [21] and Missana et al. [22] investigated the charging behaviour of portlandite and calcium silicate hydrate (CSH) phases, respectively, under conditions pertinent to these cementitious materials. They measured the electrophoretic surface potential (ζ-potential) under various chemical conditions and interpreted the results with the aid of geochemical modelling. In both CSH and portlandite, calcium adsorption was identified as the primary process influencing the surface charge. Their developed surface models also allowed to elucidate the adsorption behaviour of cationic and anionic species in these minerals [21–24].

In this study, a similar approach is proposed to analyse the variations in ettringite ζ-potential under different pH, and Ca and SO_4^{2-} concentrations. To determine the surface site density, additional insights were obtained from recent density functional theory (DFT) calculations by Colmenero et al. [25], which examined the structure of ettringite synthesised in our laboratory.

2. Materials and methods

2.1. Ettringite

Ettringite was synthesised in an anoxic glove box under a nitrogen (N_2) atmosphere following the method reported by Perkins and Palmer [26]. The synthesis involved mixing 0.02 M $Al_2(SO_4)_3{\cdot}18{\cdot}H_2O$ and 0.12 M $Ca(OH)_2$ in 1 L of ultrapure water, which had been previously boiled and N_2-sparged to minimise CO_2 contamination. To this mixture, 1 mL of 1 M Na(OH) was added. The mixture was then heated to 60 °C under continuous stirring for 48 h.

The precipitated solid was separated from the aqueous phase using a Büchner vacuum filtration funnel with a 0.2 μm filter. The solid was dried in the glove box and subsequently crushed in an agate mortar before characterisation and use in the experiments.

The synthesised solid was analysed using X-ray diffraction (XRD), Fourier-transform infrared (FTIR) spectroscopy, scanning electron microscopy (SEM), and energy-dispersive X-ray spectroscopy (X-EDS).

The powder XRD pattern was obtained using a Philips X'Pert – PRO MPD diffractometer with a Cu-Kα anticathode operating at 45 kV and 40 mA, equipped with a fixed divergence slit (0.25° size), a Ni Kβ filter, and a Scientific X′ Celerator detector. The samples were scanned from 2 to 80° 2θ with a step size of 0.02° 2θ and a time per step of 99.695 s. The Power Diffraction File from the International Centre for Diffraction Data (ICDD) was used for phase identification.

Transmission FTIR spectra were recorded on KBr-pressed discs using a Nicolet iS50 spectrometer with a DTGS KBr detector purged of CO_2 and H_2O. The spectra were analysed using Omnic 9 software.

The N_2-BET surface area of the ettringite (15.3 $m^2\ g^{-1}$) was determined using classical nitrogen adsorption/desorption isotherms obtained with a discontinuous volumetric sorptometer, Micromeritics ASAP 2020. Scanning Electron Microscopy (SEM) was performed using a JEOL 6400 JSM microscope, which was equipped with an energy-dispersive X-ray spectroscopy (X-EDS) system. This setup enabled the qualitative analysis of light elements, including boron, with a resolution of 133 eV.

2.2. Electrophoretic measurements

The electrophoretic mobility of ettringite particles suspended in different alkaline solutions (1 g L^{-1}) was measured using laser Doppler electrophoresis with a Malvern Zetamaster apparatus equipped with a He–Ne laser (λ = 633 nm). The suspensions were equilibrated for at least 1 h before measurements were taken.

The equipment recorded the movement of charged particles in a quartz cuvette under an applied electric field. Electrophoretic mobility, $\mu_e = v/E$, was determined by measuring the particle velocity (v) per unit electric field (E). The ζ-potential was calculated from μ_e using different approximations, with the Smoluchowski approximation being employed [27,28].

Ettringite persists in cement throughout different stages of aging and is exposed to complex pore water chemistries. In the initial degradation stage (Stage I), Portland cement has a high pH (13.1–13.5), dominated by alkaline elements (NaOH and KOH). As these alkalis dilute, the pH decreases and is buffered by the mineral portlandite (Stage II, pH = 12.5). Once portlandite dissolves, the pH is controlled by calcium silicate hydrates (CSH) and can drop to values around 10.5.

Therefore, the alkaline solutions in which ettringite was suspended had varying pH (10–13) and different calcium and sulphate contents, representing water at various stages of cement degradation: fresh water (Stage I), portlandite water (Stage II), and CSH (Ca/Si ~ 1) water (Stage III). Additionally, measurements were conducted with fixed pH (using NaOH) while varying the concentrations of Ca ($CaCl_2$, from 0.1 to 20 mM) or sulphate (Na_2SO_4, from 0.1 to 40 mM) to analyse their individual contributions more thoroughly.

All suspensions were prepared within the glove box, and samples for ζ-potential determination were collected with a syringe and removed from the glove box just before measurement to minimise CO_2 contamination. The quantities of calcium and sulphate were verified by chemical analysis during the electrophoretic measurements to account for any potential small dissolution of the solid during the test.

The pH, calcium, and sulphate contents of the solutions used in the experiments are summarised in Table 1. Values in parentheses in the same cell represent measurements taken after the tests (see Table 2).

2.3. Geochemical modelling

The objective of the modelling was to reproduce the charging behaviour of ettringite as a function of pH, calcium, and sulphate content. A simplified model was employed based on the classical diffuse double layer model (DLM) [20,29], which considers the presence of generic ≡SOH sites at the ettringite surface, similar to the approaches used for CSH phases [22] and portlandite [21].

In the DLM, the surface charge density (σ, C/m^2) is determined by all surface coordination reactions with cations and/or anions, and the distribution of ions in the diffuse layer is described by the Gouy-Chapman equation. The relationship between the surface charge and surface potential (Ψ) is given by the following equation:

$$\sigma = \sqrt{8 \cdot R \cdot T \cdot c \cdot \varepsilon \cdot \varepsilon_0}\sinh\left(\frac{z \cdot F \cdot \Psi}{2 \cdot R \cdot T}\right) \quad (1)$$

Table 1
Summary of the electrophoretic measurements and main characteristics of the samples.

#Test/Solution		pH	Ca (mM)	Sulphate (mM)	ζ-potential (mV)
#1	Equilibrium water	10.5 ± 0.1	14.5	17.7	−10.9 ± 3.0
#2	Na_2SO_4	12.0 ± 0.1	0 (6)	1000	−29.3 ± 5.1
#3	Stage (I) water	13.2 ± 0.1	0.5	1.4	−14.5 ± 3.0
#4	Stage (II) water	12.4 ± 0.1	15.0	0 (0.6)	20.4 ± 3.0
#5	Stage (III) water	11.3 ± 0.1	2.5	0 (0.01)	28.8 ± 3.0
#6	Synthetic water [Ca] variable (No Sulphate)	11.9 ± 0.3	0 to 20	0 (0.19)	Variable
#7	Synthetic water [SO_4^{2-}] variable (No Ca)	11.5 ± 0.1	0 (1.13)	0 to 40	Variable
#8	Synthetic water [SO_4^{2-}] variable (Fixed Ca)	11.9 ± 0.1	3.8 (3.0)	0–40	Variable
#9	Equilibrium water pH variable	10.5 to 12.5	14.5	17.7	−8.0 ± 3.0
#10	Synthetic water pH variable	10.5 to 12.5	2.3	5.7	−6.0 ± 3.0
#11	Synthetic water pH variable	10.5 to 12.5	0.7	30.8	−21.2 ± 3.0

Table 2
Parameters used for the modelling of the experimental curves.

Surface Complex		Species definition (CHESS code)	Log K Max range	Mean Log K (all the tests)
C1	SOCa[+]	1 SOH, −1 H[+], 1 Ca[2+]	−3.4 to −3.0	−3.20 ± 0.10
C2	$SOCaSO_4$[-]	1 SOH, −1 H[+], 1 Ca[2+], 1 SO_4[2-]	−1.3 to −0.7	−0.85 ± 0.20

where R is the molar gas constant, T is the absolute temperature, ε is the dielectric constant of water, Z is the valence state of the electrolyte, F is Faraday's constant, ε_0 is the vacuum permittivity, and c is the concentration of the molar electrolyte.

In the DLM approximation, the surface potential (Ψ) pertains to the diffuse layer plane or the distance of the closest approach to background electrolyte ions. Experimental determination of Ψ is challenging; therefore, an approximation based on electrokinetics or ζ-potential is commonly used.

The ζ-potential values correspond to the potential at the shear plane of the particle moving in an electric field and do not provide a direct measurement of Ψ. However, both magnitudes are approximately equal when the potentials are low (<30 mV) [28], which is often the case for cementitious materials [11].

Considering the approximations already made by Almendros-Ginestà et al. [21] and Missana et al. [22], the surface functional =SOH groups generated by cement under the (hyper)-alkaline conditions will be deprotonated, according to the reaction:

$$= SOH \Leftrightarrow_{K1} = SO^- + H^+ \quad (2)$$

Considering the DLM, the intrinsic equilibrium constant of this reaction is K_1, and the mass law equation of reaction is E.2:

$$K_1 = \frac{(= SO^-)\{H^+\}}{(= SOH)} \exp\left(-\frac{F\Psi}{RT}\right) \quad (3)$$

where {} represent the ion activity and () ion concentration.

The main reactive sites, negatively charged (=SO^-), will be able to interact with cations by reactions of this type:

$$= SO^- + M^{z+} \Leftrightarrow_{K_{C,M}} = SOM^{z-1} \quad (4)$$

The two most significant ions present in the equilibrium water of ettringite (as summarised in Table 1) are calcium and sulphate. Thus, the principal hypothesis of the model is that the formation of surface complexes involving these ions with the surface functional groups dictates the surface charge.

As observed in the CSH phases and portlandite, calcium is a crucial ion that influences the potential. Therefore, the primary reaction considered for ettringite is the formation of the complex =$SOCa^+$ (Complex 1, C1):

$$= SO^- + Ca^{2+} \Leftrightarrow_{K(C1)} = SOCa^+ \quad (5)$$

Sulphate, being an anion, is not expected to react directly with the negatively charged surface group (=SO^-). However, it can be complexed to the surface through the bridging action of calcium, resulting in the formation of the complex = $SOCaSO_4^-$ (Complex 2, C2).

$$= SOCa^+ + SO_4^{2-} \Leftrightarrow_{K(C2)} = SOCaSO_4^- \quad (6)$$

The calculation of the surface potential (Ψ) due to calcium and/or sulphate adsorption was performed using the diffuse double layer model (DLM), and these calculations were compared with the experimental ζ−potential.

Finally, the total density of the =SOH sites was taken from a previous study by Colmenero et al. [25], which investigated the structure of ettringite synthesised in our laboratory using DFT calculations. In their study, Colmenero et al. [25] identified =CaOH and =AlOH groups on surfaces perpendicular to the (010), (010), and (100) planes.

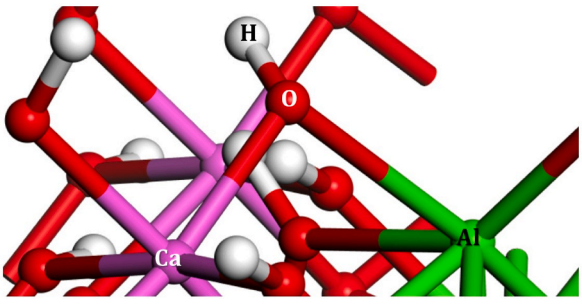

Fig. 1. Calculated structure of =SOH groups (S= Ca or Al) at the [1 0 0] ettringite surface. Colour code: Ca-violet; Al -green; O-red; S-Yellow: H-White. (For interpretation of the references to colour in this figure legend, the reader is referred to the Web version of this article.)

Fig. 1 shows examples of the calculated structures of the =CaOH and =AlOH functional groups on the [1 0 0] surface.

These two groups (=CaOH and =AlOH) are equivalent, as the OH^- ions simultaneously belong to the coordination polyhedra of Ca and Al. On the [1 0 0] surface, eight = CaOH ≠ AlOH groups were identified (two per Al atom in the surface), corresponding to surface densities of 0.033 OH^- sites/$Å^2$ or 3.3 OH^- sites/nm^2. The [010] surface can be considered equivalent to the [100] surface owing to the spatial symmetry of ettringite. Finally, on the [001] surface, three CaOH/AlOH groups were identified, with corresponding surface densities of 0.024 OH^- sites/$Å^2$ or 2.4 sites/nm^2.

For the initial testing of the geochemical model and for simplicity, we considered only a single generic surface site, =SOH, with a total surface site density calculated by DFT (9 sites/nm^2).

Modelling calculations were aided by the CHESS v3.0 code [30]. The constants were determined using a trial-and-error procedure, and the error was evaluated by sensitivity analysis and considering the results of the entire dataset (Table 1). The LogK values for the reactions forming the C1 and C2 complexes are provided according to the nomenclature of the code to facilitate data transfer between different codes.

3. Results and discussion

The XRD diffractograms and FTIR spectra of the synthesised ettringite are shown in Figs. S1 and S2 of the Supplementary Material. The XRD pattern indicates relatively pure ettringite, with a content higher than 99 wt %, matching the ettringite reference pattern 00-

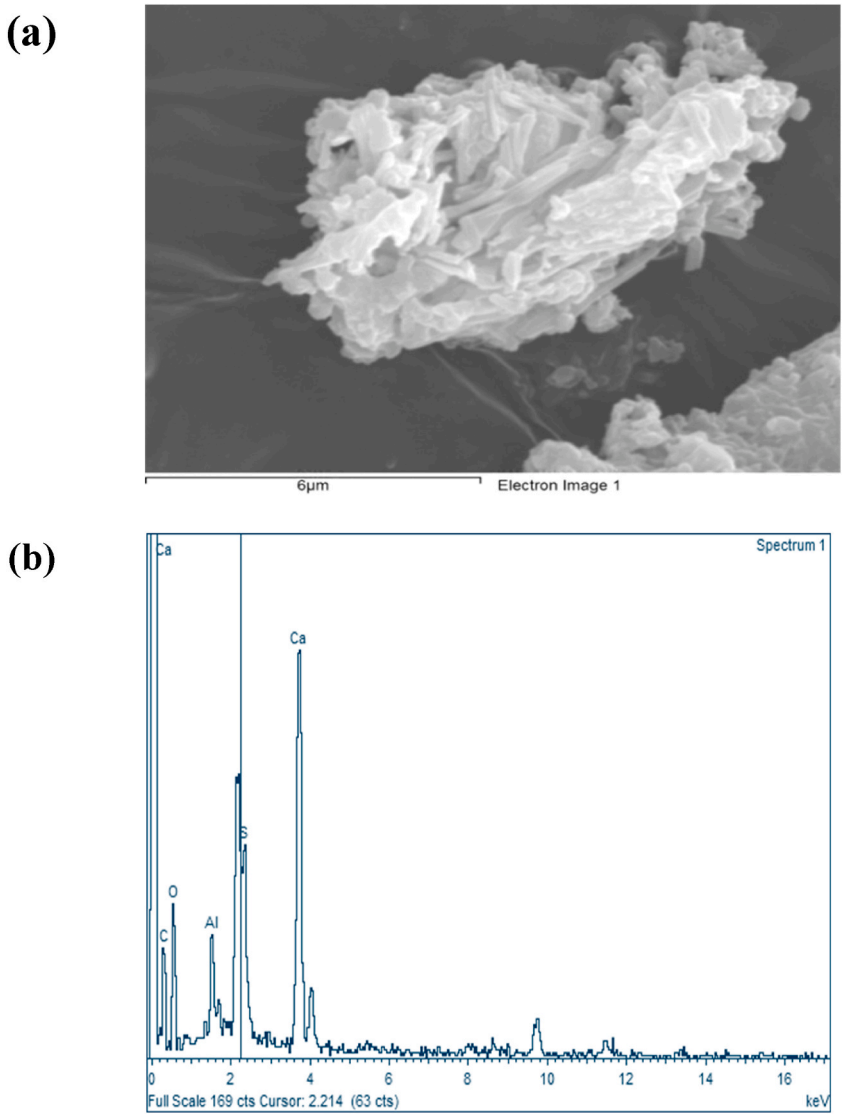

Fig. 2. a) SEM picture and b) EDS analysis of the synthetized ettringite This analysis showed that the synthetized material is pure ettringite.

013-0350 from the ICDD (Fig. S1), and traces of calcite.

The FTIR spectrum reveals major bands corresponding to H–OH (3638 cm^{-1}) and S–O (1111 and 988 cm^{-1}) stretching bands, Al–OH (2218 cm^{-1}) and H_2O (1472 and 1682 cm^{-1}) bending vibrations, and other water vibrations: water librations (l) at 873 and 855 cm^{-1}, water twisting (τ) at 615 cm^{-1}, and wagging (ω) at 542 cm^{-1}. These assignments were made using theoretical functional calculations by Colmenero et al. [25], some of which differed from other experimental studies [31,32]. Calcite was not observed in the FTIR spectrum. Contamination due to the exposure of the sample to air and CO_3^{2-} adsorption during measurement cannot be completely ruled out, as indicated by Myneni et al. [13].

Fig. 2 shows the SEM image (and the corresponding EDS analysis) of the synthesised material, which presents bladed crystals exhibiting short and thick needle-like structures with crystal lengths up to 2 μm. EDS also confirms that the synthesised mineral is pure ettringite.

The equilibrium contact water obtained during solid preparation was analysed, and its main characteristics are summarised in Table 1. The solution in equilibrium with the synthesised ettringite has a pH of 10.5. The main ions in solution are calcium and sulphate, with minor concentrations of Na and Al (0.78 and 0.11 mM, respectively)

For determining the surface charge of ettringite, electrophoretic measurements were performed by suspending the solid (1 g/L) in different aqueous solutions representing the various stages of cement degradation, to screen the possible variation of the ζ-potential under variable conditions. The results of the electrokinetic measurements in different waters are summarised in Table 1.

When the ettringite is suspended in its equilibrium water, containing 14.5 mM calcium and 17.7 mM sulphate at pH 10.5, the ζ-potential is negative (−10.9 ± 3.0 mV). In the presence of only sulphate at a high concentration (1 M Na_2SO_4 and pH 12), the ζ-potential is more negative (−29.3 ± 5.1 mV). If ettringite is suspended in a synthetic pore water representing fresh cement, Stage I, which has a relatively small content of both calcium (0.5 mM) and sulphate (1.38 mM) and a pH of 13.2, the ζ-potential is still negative (−14.5 ± 3.0 mV). However, in the water representing Stage II, at pH 12.5, where calcium is the main ion in solution (15 mM) and sulphate is absent, the ζ-potential turns positive (+20.4 ± 3.0 mV). In the water representing equilibrium with the CSH phases (Stage III, pH 11.3), where less calcium exists but no sulphate is present, the ζ-potential is still positive (+28.8 ± 3.0 mV).

This analysis demonstrates that the surface charge of ettringite can be either positive or negative, depending on the chemical conditions. Initial results suggest that both calcium and sulphate ions influence the surface charge of ettringite, acting in a competitive manner. To better understand the individual effects of calcium and sulphate on ζ-potential values, we conducted experiments where the concentration of one ion was fixed while the other was varied, following a method similar to that proposed by Medala et al. [10].

Fig. 3 shows the ζ-potential measurements of ettringite (1 g L^{-1}) in deionised water at pH 11.88 ± 0.31, with increasing calcium concentrations up to 20 mM. Sulphate was not initially added to the system, but subsequent analysis of the supernatant revealed a small amount of sulphate in all samples, with a mean value of 0.19 mM. This information was subsequently considered in the final calculations.

The addition of increasing quantities of Ca resulted in a marked increase in the surface charge of ettringite, reaching values of up to approximately +50 mV. This is consistent with the calcium adsorption at the ettringite surface, described by the formation of the surface complex C1 (Eq. (4)).

Given that the sulphate presence was negligible in the data from Fig. 3, the initial modelling run considered only the formation of complex C1 (=$SOCa^+$, Eq. (4a)), as suming null sulphate. This initial step allowed us to establish a range for the LogK(C1), which, considering the experimental errors, lies between −3.4 and −3.0, as indicated in Fig. 3.

Fig. 4 presents the ζ-potential measurements of ettringite (1 g L^{-1}) in deionised water with increasing sulphate quantities. The test shown in Fig. 4a was conducted at pH = 11.48 ± 0.09 without adding calcium. Additionally, a small amount of calcium was detected in the supernatant after contact with ettringite, averaging 1.13 mM. The tests in Fig. 4b were conducted at pH = 11.91 ± 0.12, including 3.8 mM of added calcium.

The addition of sulphate had the opposite effect to calcium on the ettringite surface charge, causing a progressive decrease in the

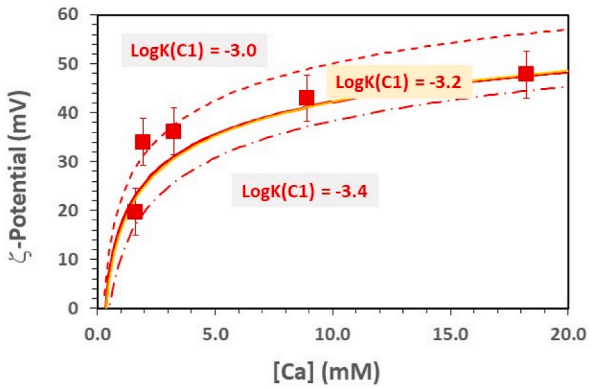

Fig. 3. ζ-potential of the ettringite (1 g L^{-1}) at pH = 11.8, as a function of the Ca content in solution. No sulphate initially present in solution. The dotted line corresponds to the limits for the LogK(C1). Continuous line corresponds to the final calculations obtained LogK(C1) = −3.2 and LogK (C2) = −1.25.

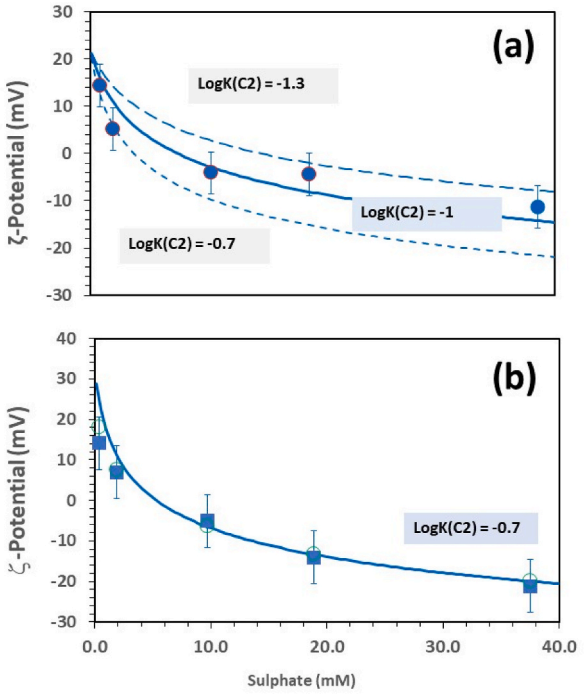

Fig. 4. ζ-potential of the ettringite (1 g L^{-1}) as a function of the sulphate content in solution. a) pH = 11.48 and no Ca present and b) pH = 11.91 with 3.8 mM Ca. In the modelling LogK(C1) was fixed to −3.2. In a) the dotted lines correspond to the maximum and minimum LogK(C2) (−0.7 and −1.3). In b) the best fit is with LogK(C2) = −0.7. Open circles correspond to point-to point calculations.

ζ-potential and reaching negative values. This indicates that sulphate also interacts with the ettringite surface, leading to the formation of a C2 complex (Eq. 4. b).

To determine the LogK range for the formation of the surface complex with sulphate (=SOCaSO$_4^-$, Eq. (4b)), the curves in Fig. 4a were simulated, considering the average calcium concentration measured from the beginning (Table 1) and fixing LogK(C1) at −3.2. As shown in Fig. 4, the LogK(C2) values fitting the experimental data ranged from −1.3 to −0.7.

Finally, considering the possible ranges for both constants obtained from the previous analysis, the model in Fig. 3 was revised to include the actual sulphate content (0.19 mM) and the respective complexation constants. The continuous line in Fig. 3 corresponds to the final model.

In summary, the best fit for the curves in Figs. 3 and 4 was achieved with the following values: LogK(C1) = −3.2 and LogK(C2) = −1.25 (Fig. 3); and LogK(C1) = −3.2 and LogK(C2) = −1 (Fig. 4a) and LogK(C1) = −3.2 and LogK(C2) = −0.7 (Fig. 4b).

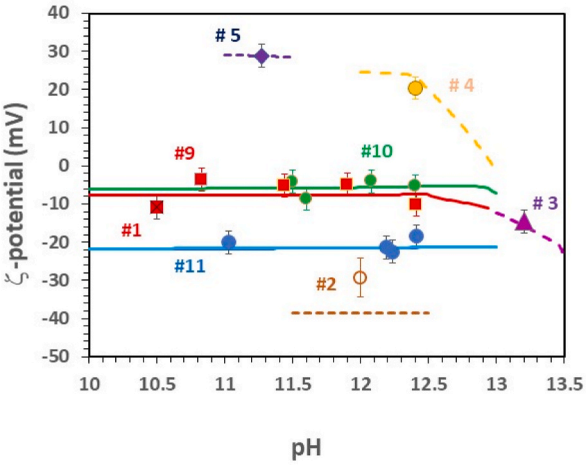

Fig. 5. ζ-potential of the ettringite (1 g L^{-1}) as a function of the pH in various solutions with different calcium and sulphate content (Table 1). The lines correspond to the modelling calculations. All the constant used for model calculations are reported in the Supplementary Material.

A further check was performed by point-to-point modelling of the individual experimental data, considering the actual pH, calcium, and sulphate content measured in each sample (not the mean). An example of these calculations is shown in Fig. 4b. Each open circle corresponds to one calculation, with all data simulated using LogK(C1, C2) within the previously determined range.

To evaluate the potential role of pH, additional tests were carried out by fixing the calcium and sulphate contents and varying the pH (from 10.5 to 13.5). The data are shown in Fig. 5. In this graph, the values of single measurements in different waters (Table 1) were also included to provide a comprehensive view of the experiments.

The results demonstrate that the ζ-potential of ettringite is minimally affected by pH, and the charge primarily depends on the relative concentration of calcium and sulphate, confirming their role as IDP.

Considering the experimental data and accounting for the actual calcium and sulphate concentrations in each experiment, all data presented in Fig. 5 were simulated considering the formation of complexes C1 and C2. The model calculations are included as lines. The LogK(C1) and LogK(C2) values used to simulate each test are reported in Table S1 of the Supplementary Material. The proposed model satisfactorily reproduces all the experimentally obtained data, and the range of variation of the proposed constants for C1 and C2 complexes is acceptable, with LogK(C1) $= -3.2 \pm 0.1$ and LogK(C2) $= -0.85 \pm 0.2$, as shown in Table S1 of the Supplementary Material. Table 2 presents a summary of the parameters used for modelling.

4. Conclusions

Under various stages of cement degradation, where pore water conditions such as pH and calcium and sulphate concentrations vary, the surface charge of ettringite can be either positive or negative. Measured ζ-potential values ranged approximately from −30 to +50 mV across different experimental conditions.

Generally, the addition of calcium increases the ζ-potential, while the addition of sulphate decreases it. The overall effect on the charge is dependent on the relative concentrations of calcium and sulphate. pH has less impact on the surface charge, underscoring the predominant roles of calcium and sulphate ions in determining the mineral's potential.

The ettringite surface charge behaviour can be explained by the formation of two surface complexes: one involving calcium and another involving sulphate. The sulphate complexation occurs through a bridging mechanism involving calcium, which creates an interrelationship between the two ions and the generic deprotonated =SOH surface sites.

This model can be used to predict the charging behaviour of ettringite under various chemical conditions.

Data availability statement

All the data supporting the conclusions of this study have been provided or are available upon request.

CRediT authorship contribution statement

Tiziana Missana: Writing – original draft, Investigation, Funding acquisition, Formal analysis, Conceptualization. **Oscar Almendros-Ginestà:** Writing – review & editing, Investigation, Data curation. **Francisco Colmenero:** Writing – review & editing, Investigation, Conceptualization. **Ana María Fernández:** Writing – review & editing, Methodology, Investigation. **Miguel García-Gutiérrez:** Writing – review & editing, Investigation, Formal analysis, Data curation.

Declaration of competing interest

The authors declare that they have no known competing financial interests or personal relationships that could have appeared to influence the work reported in this paper.

Acknowdlegements

This study was partially supported by the European Union's Horizon 2020 Research and Innovation Program under Grant Agreement no. 847593 (EURAD, CORI) and by the Spanish Ministry of Science and Innovation (PID2019–106398 GB-I00, ARNO Project).

Appendix A. Supplementary data

Supplementary data to this article can be found online at https://doi.org/10.1016/j.heliyon.2024.e36117.

References

[1] L.P. Ogorodova, Y.D. Gritsenko, D.A. Kosova, M.F. Vigasina, L.V. Melchakova, D.A. Ksenofontov, S.K. Dedushenko, Physicochemical and thermochemical study of ettringite, Geochem. Int. 59 (12) (2021) 1188–1197, https://doi.org/10.1134/S0016702921100050.
[2] A.E. Moore, H.F.W. Taylor, Crystal structure of ettringite, Acta Cryst B26 (1970) 386–393.

[3] M.L.D. Gougar, B.E. Scheetz, D.M. Roy, Ettringite and C-S-H Portland Cement phases for waste ion immobilization: a review, Waste Management 16 (4) (1996).
[4] S. Diamond, Delayed ettringite formation, Cement Concr. Compos. 18 (1996) 205–215.
[5] B. Grambow, M. López-García, J. Olmeda, M. Grivé, N.C.M. Marty, S. Grangeon, F. Claret, S. Lange, G. Deissmann, M. Klinkenberg, D. Bosbach, C. Bucur, I. Florea, R. Dobrin, M. Isaacs, D. Read, J. Kittnerová, B. Drtinová, D. Vopálka, N. Cevirim-Papaioannou, N. Ait-Mouheb, X. Gaona, M. Altmaier, L. Nedyalkova, B. Lothenbach, J. Tits, C. Landesman, S. Rasamimanana, S. Ribet, Retention and diffusion of radioactive and toxic species on cementitious systems: main outcome of the CEBAMA project, Appl. Geochem. 112 (2020) 104480.
[6] C. Colman, D. Bulteel, M. Bouarroudi, S. Elkarim, R.L. Courard, Expansion of concrete by secondary ettringite formation due to fine recycled aggregates contaminated with gypsum, Adv. Cement Res. 35 (11) (2023) 480–488.
[7] O.R. Batic, C.A. Milanesi, P.J. Maiza, S.A. Marfil, Secondary ettringite formation in concrete subjected to different curing conditions, Cement Concr. Res. 30 (9) (2000) 1407–1412.
[8] S.-S. Chen, P.K. Mehta, Note: zeta potential and surface area measurements on ettringite, Cement Concr. Res. 12 (1982).
[9] J. Plank, C. Hirsch, Impact of zeta potential of early cement hydration phases on superplasticizer adsorption, Cement Concr. Res. 37 (4) (2007) 537–542, https://doi.org/10.1016/j.cemconres.2007.01.007.
[10] M. Medala, C. Labbez, I. Pochard, A. Nonat, Ettringite surface chemistry: interplay of electrostatic and ion specificity, J. Colloid Interface Sci. 354 (2) (2011) 765–770, https://doi.org/10.1016/j.jcis.2010.11.031.
[11] I. Pointeau, P. Reiller, N. Macé, C. Landesman, N. Coreau, Measurement and modeling of the surface potential evolution of hydrated cement pastes as a function of degradation, J. Colloid Interface Sci. 300 (1) (2006) 33–44, https://doi.org/10.1016/j.jcis.2006.03.018.
[12] S. Myneni, S. Traina, T. Logan, G. Waychunas, Oxyanion behavior in alkaline environments: sorption and desorption of arsenate in ettringite, Environ. Sci. Technol. 31 (1997) 1761–1768. https://pubs.acs.org/sharingguidelines.
[13] S.C.B. Myneni, S.J. Traina, G.A. Waychunas, T.J. Logan, Vibrational spectroscopy of functional group chemistry and arsenate coordination in ettringite, Geochem. Cosmochim. Acta 62 (21/22) (1998) 3499–3514.
[14] I. Bonhoure, I. Baur, E. Wieland, C.A. Johnson, A.M. Scheidegger, Uptake of Se(IV/VI) oxyanions by hardened cement paste and cement minerals: an X-ray absorption spectroscopy study, Cement Concr. Res. 36 (1) (2006) 91–98, https://doi.org/10.1016/j.cemconres.2005.05.003.
[15] M. Ochs, D. Mallants, L. Wang, in: Topics in Safety, Risk, Reliability and Quality Radionuclide and Metal Sorption on Cement and Concrete, 2016. ISBN 978-3-319-23651, http://www.springer.com/series/6653.
[16] B. Guo, K. Sasaki, T. Hirajima, Selenite and selenate uptaken in ettringite: immobilization mechanisms, coordination chemistry, and insights from structure, Cement Concr. Res. 100 (2017) 166–175, https://doi.org/10.1016/j.cemconres.2017.07.004.
[17] D. Hou, T. Li, Q. Han, J. Zhang, Insight on the sodium and chloride ions adsorption mechanism on the ettringite crystal: structure, dynamics and interfacial interaction, Comput. Mater. Sci. 153 (2018) 479–492, https://doi.org/10.1016/j.commatsci.2018.07.021.
[18] C. Fan, B. Wang, Y. Xu, Solidification/stabilization and immobilization mechanism of Pb(II) and Zn(II) in ettringite, Cement Concr. Res. 174 (2023), https://doi.org/10.1016/j.cemconres.2023.107350.
[19] R. Dohrmann, D. Genske, O. Karnland, S. Kaufhold, L. Kiviranta, S. Olsson, M. Plötze, T. Sandén, P. Sellin, D. Svensson, M. Valter, Interlaboratory CEC and exchangeable cation study of bentonite buffer materials: II. alternative methods, Clay Clay Miner. 60 (2) (2012) 176–185, https://doi.org/10.1346/CCMN.2012.0600207.
[20] C.-P. Huang, W. Stumm, Specific adsorption of cations on hydrous "~-AI203, J. Colloid Interface Sci. 43 (2) (1973) 409–419.
[21] O. Almendros-Ginestà, T. Missana, M. García-Gutiérrez, U. Alonso, Analysis of radionuclide retention by the cement hydrate phase portlandite: a novel modelling approach, Prog. Nucl. Energy 159 (2023), https://doi.org/10.1016/j.pnucene.2023.104636.
[22] T. Missana, M. García-Gutiérrez, M. Mingarro, U. Alonso, Analysis of barium retention mechanisms on calcium silicate hydrate phases, Cement Concr. Res. 93 (2017) 8–16, https://doi.org/10.1016/j.cemconres.2016.12.004.
[23] T. Missana, M. García-Gutiérrez, M. Mingarro, U. Alonso, Comparison between cesium and sodium retention on calcium silicate hydrate (C–S–H) phases, Appl. Geochem. 98 (2018) 36–44, https://doi.org/10.1016/j.apgeochem.2018.09.007.
[24] T. Missana, M. García-Gutiérrez, M. Mingarro, U. Alonso, Selenite retention and cation coadsorption effects under alkaline conditions generated by cementitious materials: the case of C-S-H phases, ACS Omega 4 (8) (2019) 13418–13425, https://doi.org/10.1021/acsomega.9b01637.
[25] F. Colmenero, A.M. Fernández, O. Almendros-Ginestà, T. Missana, Density functional theory study of the crystal structure and infrared spectrum of a synthetized ettringite mineral, Minerals 14 (8) (2024) 824, https://doi.org/10.3390/min14080824.
[26] R.B. Perkins, C.D. Palmer, Solubility of ettringite (Ca 6 [Al(OH) 6] 2 (SO 4) 3 26H 2 O) at 5-75°C, Geochem. Cosmochim. Acta 63 (13/14) (1999) 1969–1980.
[27] R.J. Hunter, Zeta Potential in Colloid Science. Principle and Applications, Academic Press, 1981. ISBN 978-0-12-361961-7.
[28] A.V. Delgado, F. Gonzalez-Caballero, R.J. Hunter, L.K. Koopal, J. Lyklema, Measurement and interpretation of electokinetic phenomena, Journal of Colloids and Interface Science 309 (2007) 194–224.
[29] D.A. Dzombak, F. Morel, Surface Complexation Modelling: Hydrous Ferric Oxide, Wiley, 1990.
[30] J. Van der Lee, J. de Windt, User's manual CHESS tutorial and cookbook updated for version 3.0 the user's guide for the geochemical model CHESS and its graphic user interface, JCHESS. Ecole des Mines de Paris (2002). LHM/RD/02/13.
[31] E. Scholtzová, D. Tunega, S. Speziale, Mechanical properties of ettringite and thaumasite - DFT and experimental study, Cement Concr. Res. 77 (2015) 9–15, https://doi.org/10.1016/j.cemconres.2015.06.008.
[32] Y. Lou, Z. Ye, S. Wang, S. Liu, X. Cheng, Influence of synthesis methods on ettringite dehydration, Journal of Thermal Analysis and Calorimetry 135 (4) (2019) 2031–2038, https://doi.org/10.1007/s10973-018-7391-8.